Clean Energy from Poplar and Plastic Mix Valorization in a Gas Turbine with CO2 Capture Process

Nela Slavu * and Cristian Dinca *

Posted Date: 12 September 2023

doi: 10.20944/preprints202309.0753.v1

Keywords: CO2 capture; gasification; gas turbine; plastics; poplar

Article

Clean Energy from Poplar and Plastic Mix Valorization in a Gas Turbine with CO_2 Capture Process

Nela Slavu [1,2,*] and Cristian Dinca [1,2,*]

[1] Energy Generation and Use Department, Faculty of Power Engineering, National University of Science and Technology Politehnica Bucharest, 313 Splaiul Independentei, 060042 Bucharest, Romania;
[2] Academy of Romanian Scientists, Ilfov 3, 050044 Bucharest, Romania
* Correspondence: nela.slavu@upb.ro (N.S); cristian.dinca@upb.ro (C.D.).

Abstract: The scope of this paper is to use plastic waste through the gasification process for producing electricity with low carbon dioxide emissions. Worldwide, plastic production increased, reaching 390 million tons in 2021, compared with 1.5 million tons in 1950. It is known that plastic incineration generates approximately 400 million tons of CO_2 annually, and consequently, new solutions for more efficient plastics reuse in terms of emissions generated are still expected. One method is to use plastic waste in a gasifier unit and the syngas generated in a gas turbine for electricity production. The co-gasification process (plastic waste with biomass) was analysed in different ratios. Gasification was carried out with air for an equivalent ratio (ER) between 0.10-0.45. The volume concentration of CO_2 in syngas ranged from 2-12%, with the highest value obtained when poplar content in the mix was 95%. In this study, the option of pre- and post-combustion integration of the chemical absorption process (CAP) was investigated. Thus, CO_2 emissions have decreased by 90% compared with the case without CO_2 capture. By integrating the capture process, the global efficiency has reduced with 5.5 – 6.1 percentage points in a post-combustion case, according to the plastic content in the mix.

Keywords: CO_2 capture; gasification; gas turbine; plastics; poplar

1. Introduction

The pyrolysis and gasification processes are thermal treatment methods that take place in successive stages from drying to subsequent devolatilization, gasification of the coke, and finishing with partial oxidation. There is no clear distinction between these phases from the studies carried out so far, so they can be run simultaneously over specific temperature ranges in real processes. The process of devolatilization shall be carried out in the absence of oxygen in the temperature range 350 to 850 °C. Depending on the heating rate, the stationary time in the chemical reaction area, and the feed content, the resulting gasification products can be classified as follows: (a) solids and mainly coke; (b) liquids consisting of heavy hydrocarbons, water, different types of oils and tar; And c) gaseous components such as H_2, CO, CO_2, C_xH_y, H_2O, etc. After that, secondary reactions may occur in which the resulting volatiles participate in the formation of the various products [1–5].

After the pyrolysis process, the gasification process takes place. Using a gasification agent (steam, air, or oxygen) allows the conversion of larger molecules into stable gases such as CO, CO_2, C_xH_y, H_2, water, tar, and ash [6,7]. The gasification process takes place at higher temperatures, often exceeding 1200 °C. Following the two pyro-gasification processes, the resulting product is a synthetic gas with a temperature of not more than 1000 °C and a composition based on gases such as CO, H_2, CO_2, C_xH_y, and other gases inert gases generated according to the gasification agent used [8]. Synthesis gas can be utilised in different types of energy installations, such as internal combustion engines or thermal engines, of which gas turbines are most known for electricity generation [9,10]. In addition, several processes can be integrated to improve the quality of synthesis gas, such as a water

 doi:10.20944/preprints202309.0753.v1

gas shift reactor (WGS) used for the conversion of carbon monoxide into hydrogen or carbon dioxide capture processes [11].

The mixture's compound has a crucial contribution in determining the composition of the synthesis gas and determining the optimal process parameters. The gasification agent also plays a significant role in setting operational parameters. In this study, the gasification agent used was air, in which case the optimal ER (ratio equivalent) ratio was established.

Given the sharp increase in plastic waste resulting from anthropogenic activities, sustainable reduction has become a global goal. This waste can be recovered by its gasification for producing a synthesis gas with improved properties (e.g. H_2/CO ratio) [12]. The present study analysed the mix of plastic (PP) and wood biomass poplar (P) in various proportions. The syngas was used as fuel in a gas turbine with a power installed of 5 MW for electricity production.

2. Methods

2.1. Gasification process description

The gasification process has the role of transforming different solid components from the feed-in gaseous compounds by using a gasification agent; in this case, the air was used as a gasification agent. The equations presented below describe the stages that occur during the gasification process [9].

$$C + \frac{1}{2}O_2 \rightarrow CO\ (-111\ MJ/kmol) \quad (1)$$

$$C + \frac{1}{2}O_2 \rightarrow CO_2\ (-283\ MJ/kmol) \quad (2)$$

$$H_2 + \frac{1}{2}O_2 \rightarrow H_2O\ (-242\ MJ/kmol) \quad (3)$$

$$C + H_2O \rightarrow CO + H_2\ (water\ gas\ reaction, +131\ MJ/kmol) \quad (4)$$

$$C + CO_2 \rightarrow 2CO\ (boudouard\ reaction, +172\ MJ/kmol) \quad (5)$$

$$C + 2H_2 \rightarrow CH_4\ (methanation\ reaction, -75\ MJ/kmol) \quad (6)$$

$$CO + H_2O \rightarrow CO_2 + H_2\ (water\ gas\ shift\ reaction, -41\ MJ/kmol) \quad (7)$$

$$CH_4 + H_2O \rightarrow CO + 3H_2\ (steam\ methane\ reforming\ reaction, -206\ MJ/kmol) \quad (8)$$

In the current study, a mix between plastic – PP and wood – poplar was used. The feedstock composition, in dry basis (db), for each case is presented in Table 1 [13,14]. The lower heating value (LHV) in kJ/kg was given by equation 9.

$$LHV = (81.3 * C + 243 * H + 15 * N - 25.3 * O + 45.6 * S) * 4.184\ (kJ/kg) \quad (9)$$

The cases studied are the following:

1. Case 1. P-PP mix gasification without CO_2 capture process;
2. Case 2. P-PP mix gasification with pre-combustion CO_2 capture process;
3. Case 3. P-PP mix gasification with post-combustion CO_2 capture process.

Preprints (www.preprints.org) | NOT PEER-REVIEWED | Posted: 12 September 2023 doi:10.20944/preprints202309.0753.v1

Table 1. Main data for feedstock composition[db]*.

Composition	Biomass P**	Plastic PP***	Mix poplar with plastic (polypropylene) P-PP, % wt.					
			95-5	90-10	85-15	80-20	75-25	70-30
C – Carbon, wt.%	50.02	83.74	51.71	53.39	55.08	56.76	58.45	60.14
H – Hydrogen, wt.%	6.28	13.71	6.65	7.02	7.39	7.77	8.14	8.51
O – Oxygen, wt.%	42.17	0.98	40.11	38.05	35.99	33.93	31.87	29.81
N – Nitrogen, wt.%	0.19	0.02	0.18	0.17	0.16	0.16	0.15	0.14
S – Sulphur, wt.%	0.02	0.08	0.02	0.03	0.03	0.03	0.04	0.04
A – Ash, wt.%	1.32	1.47	1.33	1.34	1.35	1.35	1.35	1.36
LHV, MJ/kg	18.95	42.34	20.12	21.29	22.46	23.63	24.80	25.97

* db – dry basis; ** P – poplar; *** PP – polypropylene.

For all three cases, the a-f cases are considered, in which the poplar and plastic content varies in the feedstock mix: a. P 95% + PP 5%; b. 90% + PP 10%; c. P 85% + PP 15%; d. P 80% + PP 20%; e. P 75% + PP 25%; f. P 70% + PP 30%.

All described processes were simulated in the ChemCAD software to determine the energy and mass balances and technical effects of CO_2 capture process integration as well.

The composition of the synthetic gas was determined after different stages: after gasification unit, after solid separator unit, and after water separator facility. The illustrative chart of the gasification process is presented in Figure 1, and the essential information of the process simulation are posted in Table 2.

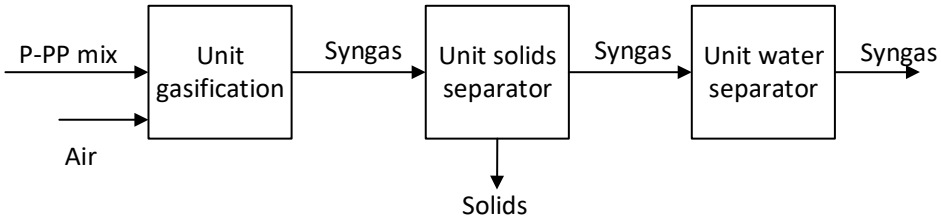

Figure 1. Diagram of the gasification process.

For establishing the optimum ER (equation 10), the cold gas efficiency (CGE) was calculated based on equation 11. B_s and B_f represent the syngas and feedstock flow, in kg/h, while LHV_s and LHV_f represent the LHV, in kJ/kg for syngas and feedstock.

$$ER = \frac{B_{real\_air}}{B_{stoichiometric\_air}} \left[\frac{\frac{kg_{real\_air}}{h}}{\frac{kg_{stoichiometric\_air}}{h}} \right] \quad (10)$$

where the B_{real_air} and $B_{stoichiometric\_air}$ represent the real and stoichiometric air flow, in kg/h.

$$CGE = \frac{B_s * LHV_s}{B_f * LHV_f} * 100\ [\%] \quad (11)$$

Table 2. Main data for gasification process simulation.

Process type	Adiabatic
Oxidizing agent	Air
P-PP flow mix, kg/h	1
Temperature, °C	600-1200
Pressure, bar	1.013
ER, [-]	0.1; 0.15; 0.2; 0.25; 0.3; 0.35; 0.4; 0.45

Preprints (www.preprints.org) | NOT PEER-REVIEWED | Posted: 12 September 2023 doi:10.20944/preprints202309.0753.v1

2.2. Syngas decarbonization

To improve the quality of the synthetic gas, the CAP was integrated pre-, and post-combustion. In the pre-combustion variant, the CAP for removing the CO_2 was integrated after the gasification process and the water separation unit. In the post-combustion variant, the CO_2 capture process was integrated after the syngas combustion. The results were obtained in the ChemCAD tool using the Peng Robinson thermodynamic model [15,16]. Figure 2 presents the chemical absorption process that could be used both in pre-, or post-combustion cases [17,18]. Ethanolamine (MEA) in a weight content of 30 % was used as an alkanolamines solution for CO_2 removal. The efficiency of CO_2 removal was considered 90 %, and the lean loading solvent (γ_{lean}) was considered 0.21 $kmol_{CO2}/kmol_{MEA}$ for all cases analysed [19,20].

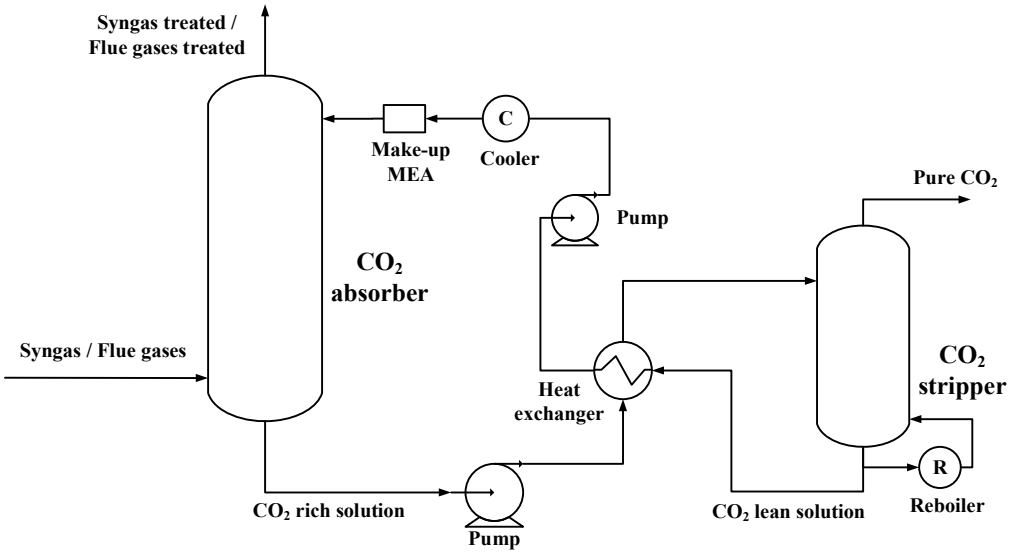

Figure 2. CO_2 capture process.

The CO_2 capture process is characterised by the L/G ratio, which is the ratio of the flow rate of chemical solvent used to the flow rate of the syngas/flue gases [20,21]. It is also characterized by the amount of specific heat energy required in the chemical solvent regeneration process [22], which is calculated with the following equation:

$$Heat\_duty = \frac{P_{thermal\_CO2capture}}{B_{CO2\_captured}} \; [GJ/t_{CO2}] \tag{12}$$

where: $P_{thermal\_CO2capture}$ - represents the heat requested in the regeneration process, in MJ/h; $B_{CO2\_captured}$ - represents the CO_2 flow captured, in kg/h.

In this study, the heat requested in the regeneration process was obtained by cooling the flue gases at the outlet of the gas turbine from 540 °C to 120°C. The available heat flow recovered from flue gases to obtain a steam (p = 5 bar and T = 424.25 K) was 9 209 MJ/h (Figures 4 and 5). However, the net heat flow used directly in the solvent regeneration was lower than the heat flow available, 434 – 776 MJ/h for pre-combustion and 5 318 – 6 102 MJ/h post-combustion case. Therefore, the heat available after the solvent regeneration was used for air and syngas heating before the combustion chamber.

2.3. Syngas conversion in electricity

A gas turbine type SGT-100, which can be used in simple or combined cycles, with a power of 5 MW, was used to valorize the produced syngas. Its characteristics are shown in Table 3 [23]. Schematic diagrams for the three cases analysed are shown in Figures 3–5. The net plant efficiency was determined in 2 variants: a) including the gas turbine only, and considering as input the chemical heat from syngas (LHV_s), equation 13; and b) for the whole process including the gasification process,

Preprints (www.preprints.org) | NOT PEER-REVIEWED | Posted: 12 September 2023 doi:10.20944/preprints202309.0753.v1

and considering as input the chemical heat of mix feedstock flow (LHV_f), equation 14. The CO_2 emission factor was determined with equation 15.

Table 3. Main data for gasification process simulation.

Type	SGT-100
Power, MW	5
Speed, rpm	17,384
Pressure ratio, -	14
Flue gases temperature at the gas turbine inlet, °C	~ 544
Flue gases flow, kg/s	up to 19.5

$$\eta_{GT} = \frac{P_{GT} - P_{comp}}{B_s * LHV_s + Q_{ex\_capture}} * 100\ [\%] \quad (13)$$

$$\eta_{GGT} = \frac{P_{GT} - P_{comp}}{B_f * LHV_f + Q_{ex\_capture}} * 100\ [\%] \quad (14)$$

where: P_{GT} - represents the gas turbine power, in MW; P_{comp} - represents the compressor power, in MW; $Q_{ex\_capture}$ - represents the required heat recovered from the flue gas, in MW.

$$f_{CO2} = \frac{M_{CO2}}{E_g}, [\mathrm{kgCO_2/MWh}] \quad (15)$$

where: M_{CO2} - represents the CO_2 amount generated, in kg/year; E_g - represents the electricity produced, in MWh/year.

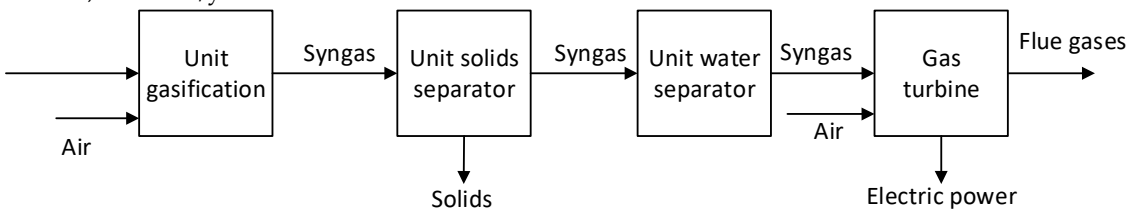

Figure 3. Diagram of the syngas conversion in electricity without CO_2 capture process.

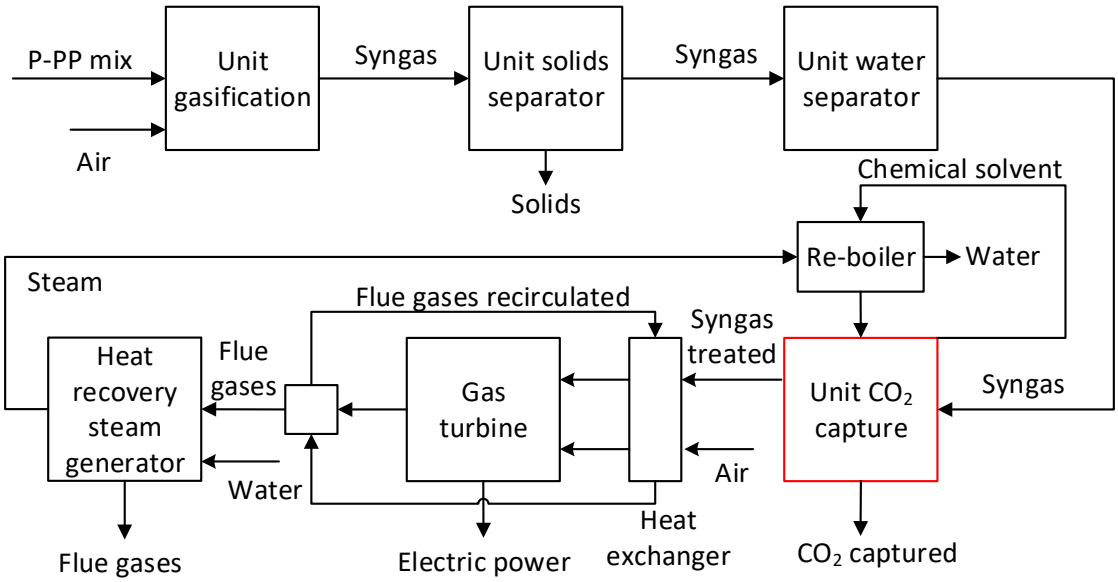

Figure 4. Diagram of the syngas conversion in electricity with pre-combustion CO_2 capture.

Preprints (www.preprints.org) | NOT PEER-REVIEWED | Posted: 12 September 2023 doi:10.20944/preprints202309.0753.v1

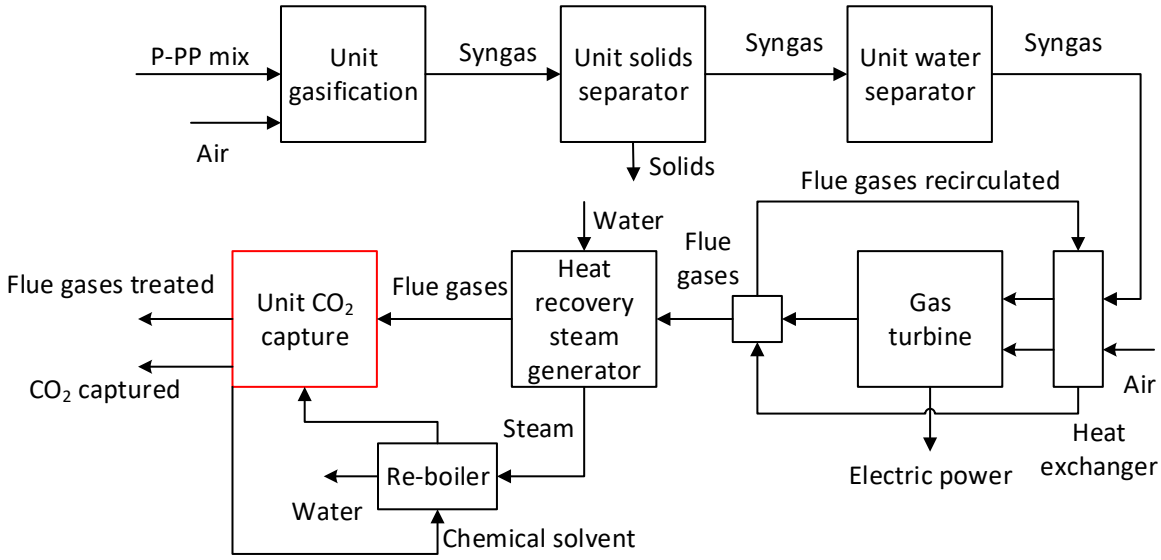

Figure 5. Diagram of the syngas conversion in electricity with post-combustion CO_2 capture process.

3. Results and discussion

3.1. Influence of ER ratio on the gasification process

The quantity of air injected into the gasifier unit significantly impacts the reaction products. Thus, the influence of the ER ratio on the syngas content produced, the LHV of the syngas, and the CGE was analysed for all mix cases considered.

In Table 4, the syngas composition is shown by gasification, solid separation, and water separation units for Case 1a.

The H_2 and CO concentrations in the syngas increased up to an ER value of 0.35 and decreased tendency after a higher ER ratio. Consequently, the efficiency of the syngas has the best value for this ER ratio after the gasification process, even though the LHV of the syngas decreases with ER ratio increases (Figure 6).

Considering that for the other mix cases analysed (Case 1b-f) the same interpretations of the results were obtained for the syngas composition; they are presented in Table 4 only for Case 1a.

Table 4. Syngas composition after gasification, solid separation, and water separation units for Case 1a.

ER	0.1	0.15	0.2	0.25	0.3	0.35	0.4	0.45
Syngas composition after gasification unit, mol fraction								
H_2	0.1677	0.1761	0.1781	0.1772	0.1746	0.1672	0.1294	0.0942
CH_4	0.0206	0.0135	0.0096	0.0072	0.0055	0.0021	0.0000	0.0000
N_2	0.1987	0.2681	0.3262	0.3757	0.4183	0.4534	0.4847	0.5141
CO	0.0851	0.1319	0.1747	0.2127	0.2463	0.2670	0.2526	0.2357
CO_2	0.0657	0.0627	0.0578	0.0521	0.0464	0.0407	0.0373	0.0377
H_2O	0.1544	0.1241	0.1014	0.0839	0.0699	0.0660	0.0927	0.1153
H_2S	0.0001	0.0001	0.0001	0.0001	0.0001	0.0001	0.0000	0.0000
Char	0.3026	0.2188	0.1478	0.0873	0.0353	0.0000	0.0000	0.0000
SiO_2	0.0052	0.0047	0.0043	0.0039	0.0037	0.0034	0.0032	0.0030
Syngas composition after solids separator unit, mol fraction								
H_2	0.2423	0.2267	0.2101	0.1950	0.1817	0.1678	0.1298	0.0945
CH_4	0.0297	0.0174	0.0113	0.0079	0.0057	0.0021	0.0000	0.0000
N_2	0.2870	0.3453	0.3848	0.4134	0.4352	0.4550	0.4863	0.5157
CO	0.1230	0.1699	0.2060	0.2341	0.2563	0.2679	0.2534	0.2364

Preprints (www.preprints.org) | NOT PEER-REVIEWED | Posted: 12 September 2023 doi:10.20944/preprints202309.0753.v1

CO_2	0.0949	0.0808	0.0681	0.0573	0.0483	0.0409	0.0374	0.0378
H_2O	0.2230	0.1598	0.1196	0.0923	0.0728	0.0662	0.0930	0.1156
H_2S	0.0001	0.0001	0.0001	0.0001	0.0001	0.0001	0.0000	0.0000
Syngas composition after solids separator unit, mol fraction								
H_2	0.3119	0.2699	0.2386	0.2148	0.1959	0.1797	0.1431	0.1068
CH_4	0.0382	0.0207	0.0129	0.0087	0.0062	0.0023	0.0000	0.0000
N_2	0.3694	0.4109	0.4370	0.4554	0.4694	0.4872	0.5362	0.5831
CO	0.1583	0.2022	0.2340	0.2579	0.2764	0.2869	0.2794	0.2673
CO_2	0.1221	0.0962	0.0774	0.0632	0.0521	0.0438	0.0413	0.0427
H_2S	0.0001	0.0001	0.0001	0.0001	0.0001	0.0001	0.0001	0.0001

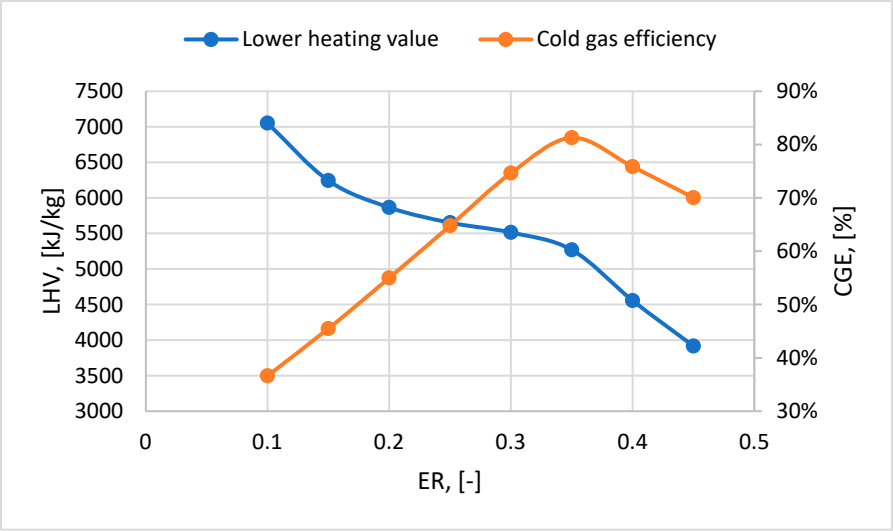

Figure 6. LHV and CGE variation according to ER for Case 1a.

The LHV ranges from 3 900-8 500 kJ/kg depending on the ER ratio and the raw material mix used in the gasification process. It is observed that (Figure 7) LHV decreases with the introduction of more air into the gasification reactor due to the lower concentration of H_2 in the syngas produced, even if the CO concentration is increasing. Increasing the content of plastic in the mix has a positive impact on the LHV value (with a percentage increase between 1-5%), obtaining the highest value at a plastic content in the mix of 30% regardless of the ER ratio.

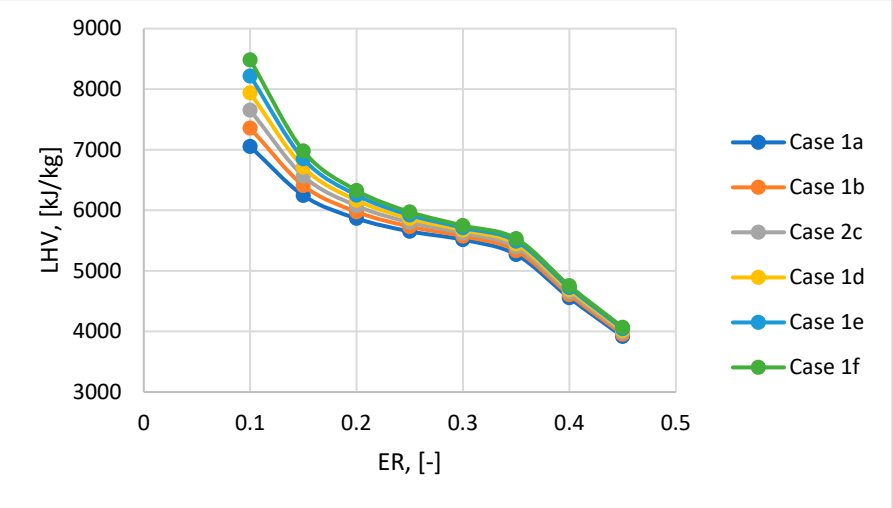

Figure 7. LHV variation according to ER.

Preprints (www.preprints.org) | NOT PEER-REVIEWED | Posted: 12 September 2023 doi:10.20944/preprints202309.0753.v1

Figure 8 shows the CGE variation. The best results are obtained at the ER ratio of 0.35. For this ratio, the CGE is between 81.3-82%. The CGE value starts to decrease after an ER ratio of 0.35 due to the more drastic decrease of LHV (LHV at an ER ratio of 0.4 is 14% lower than LHV at an ER ratio of 0.35), even though the flow rate of syngas generated is higher. Case 1f showed the best values in terms of CGE, as in the LHV case.

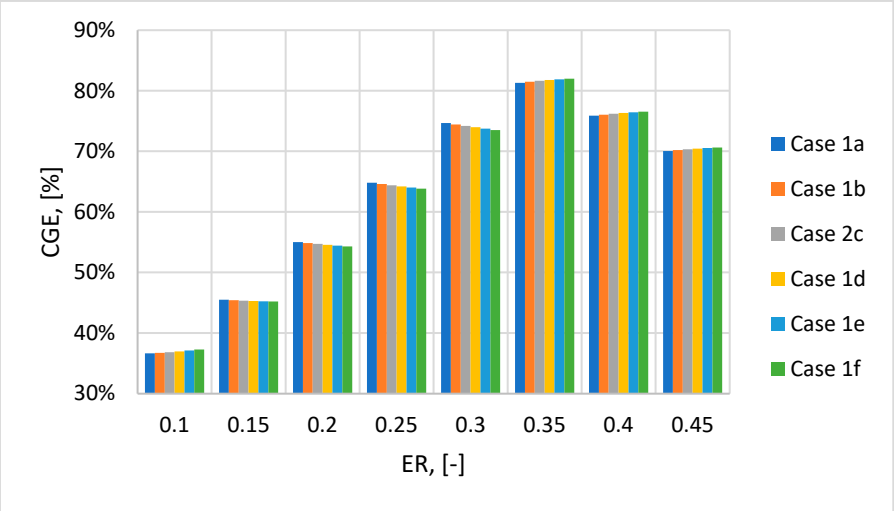

Figure 8. CGE variation according to ER.

H_2/CO is the ratio of the number of moles of hydrogen to the number of moles of carbon monoxide in the syngas, with values up to 0.73 for Case 1f. It means that the concentration value for H_2 is the highest in this case, and the value for CO is the lowest. On the other hand, the CO_2 concentration decreases as the concentration of plastic increases in the mixture. Considering that the CGE was obtained at an ER ratio of 0.35, the optimal ER ratio is considered in the following analyses. Table 5 shows the results obtained after the gasification process for all the mix cases analysed for this ER ratio.

Table 5. Results of gasification process for ER = 0.35 – Case 1.

Case	1a	1b	1c	1d	1e	1f
ER, -	0.35	0.35	0.35	0.35	0.35	0.35
Gas temperature, °C	40	40	40	40	40	40
Syngas flow	3.10	3.25	3.40	3.55	3.70	3.85
LHV, kJ/kg	5 269	5 333	5 391	5 443	5 490	5 532
H_2/CO, -	0.63	0.65	0.67	0.69	0.71	0.73
CGE, %	81.30	81.47	81.63	81.77	81.89	81.98
Syngas composition, mole %						
H_2	17.97	18.42	18.83	19.21	19.55	19.87
CH_4	0.23	0.25	0.28	0.30	0.32	0.34
N_2	48.72	49.03	49.29	49.53	49.74	49.94
CO	28.69	28.41	28.14	27.88	27.63	27.38
CO_2	4.38	3.88	3.45	3.08	2.75	2.46
H_2S	0.01	0.01	0.01	0.01	0.01	0.01

3.2. Energetic valorisation of syngas in a gas turbine

After the gasification process and syngas treatment (removal of solid particles, water), the syngas was used to produce electricity in a gas turbine with a power of 5 MW for all the mix cases studied (a-f). The flue gases temperature at the turbine inlet was about 1 200 °C and at the outlet about 540 °C. The ratio between the flow rate required for combustion and the flow rate of the syngas

Preprints (www.preprints.org) | NOT PEER-REVIEWED | Posted: 12 September 2023 doi:10.20944/preprints202309.0753.v1

was between 4.28-4.55 kg_{air}/kg_{syngas}. Thus, to have the same gas turbine power, with increasing plastic content in the mix, the required syngas flow rate is lower due to better LHV and CGE in this Case (1f). Therefore, just to exemplify, the net plant efficiency is the highest in Case 1f, 41.06% or 33.7%, with the lowest emission factor of 907.44 $kgCO_2/MWh$ (Table 6).

Table 6. Results of syngas use in a gas turbine – Case 1.

Case	1a	1b	1c	1d	1e	1f
Gas turbine power, MW	5	5	5	5	5	5
Syngas flow, kg/h	4 226.19	4 166.87	4 122.22	4 079.09	4 046.16	4 011.36
Air flow, kg/h	18 105.73	18 166.44	18 181.29	18 213.95	18 214.20	18 243.19
Combustion chamber temperature, °C	1 202.88	1 201.25	1 201.68	1 201.06	1 201.89	1 201.19
Flue gases temperature at the gas turbine outlet, °C	543.71	542.15	541.99	541.20	541.38	540.62
Flue gases flow, kg/h	22 331.94	22 333.32	22 303.52	22 293.05	22 260.38	22 254.56
η_{GT}, %	41.01	41.04	41.04	41.05	41.05	41.06
η_{GGT}, %	33.34	33.44	33.51	33.57	33.61	33.66
CO_2 emission factor, $kgCO_2/MWh$	1 016.55	989.18	965.43	943.92	924.98	907.44
Flue gases composition, wt. %						
H_2	0.02	0.02	0.02	0.02	0.02	0.02
O_2	13.03	13.10	13.12	13.16	13.17	13.21
N_2	72.95	73.16	73.33	73.49	73.62	73.75
CO_2	11.55	11.22	10.97	10.72	10.52	10.32
H_2O	2.45	2.50	2.56	2.61	2.66	2.70

Tables 7 and 8 show the results obtained for L/G ratio and the quantity of heat energy to regenerate the solvent. The capture efficiency in both cases (Case 2 and 3) was 90%. The L/G ratio did not exceed 1 kgsolvent/kgsyngas or kgsolvent/kgflue_gases and the specific heat duty was varied between 2.521-2.636 GJ/tCO_2.

Considering that the CO_2 concentration in synthetic gas decreased as the plastic content increased in the feedstock, the L/G ratio decreased (Figure 9). The specific heat required for solvent regeneration is approximately the same for all cases. Thus, the plastic PP content in the feedstock mix doesn't influence the heat consumption for solvent regeneration. As it can see in Figure 10, the LHV has increased from 5 269-5 532 kJ/kg in Case 1 to 5 687-5 778 kJ/kg in Case 2.

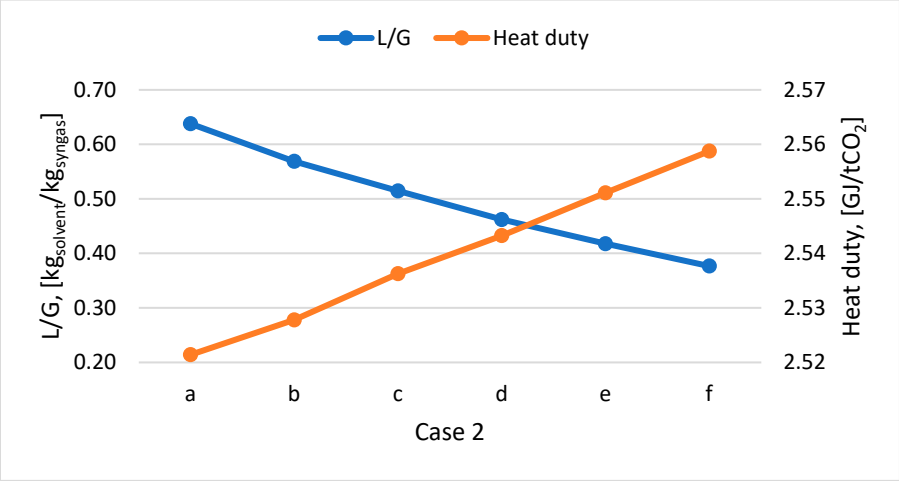

Figure 9. L/G ratio and heat duty variation according to PP content in the mix for Case 2.

Preprints (www.preprints.org) | NOT PEER-REVIEWED | Posted: 12 September 2023 doi:10.20944/preprints202309.0753.v1

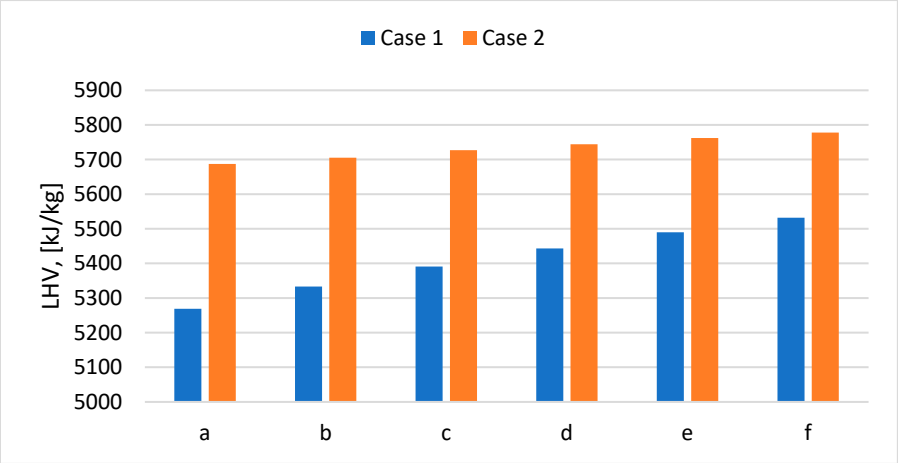

Figure 10. LHV according to PP content in the mix for Cases 1 and 2.

The amount of solvent is significantly lower in the pre-combustion case (Case 2) than in the post-combustion case (Case 3) for the same CO_2 capture efficiency (90%) due to a lower amount of CO_2 in the stream. For cases a-f, the L/G ratio decreases with increasing plastic concentration in the mix for both cases studied (Figure 11). Specific heat duty does not differ significantly, regardless of how the CO_2 capture process is integrated. For example, for Case 2a an amount of 2.521 GJ/tCO_2 is needed, and in Case 2b an amount of 2.614 is needed, with an increase of 3.69%. Specific heat duty increases with increasing plastic content in the mix (Figure 12).

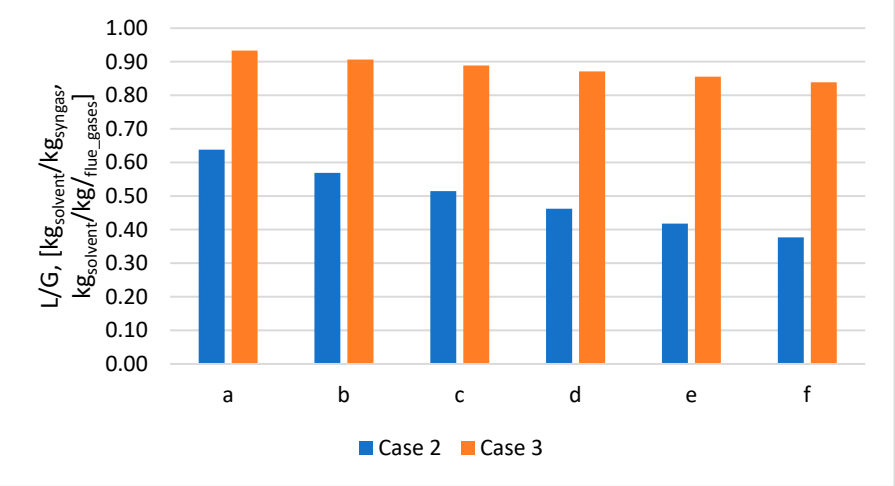

Figure 11. Variation of the L/G ratio according to PP content in the mix for Cases 2 and 3.

The water consumption for the CO_2 capture process varies between 3 442.72-6 241.96 kgH_2O/year in Case 2. The lowest water consumption value corresponds to Case 2f when the plastic content in the mix is 30% due to the lower amount of CO_2 captured per year because less feedstock mix is needed to produce the same power. In Case 2, the water consumption is significantly lower than in Case 3 (42 099.81-47 332.05 kgH_2O/year) due to the lower gas stream debit treated in the CO_2 capture unit. In both cases, the water footprint is approximately 3 kgH_2O/t$CO_{2_captured}$.

The results obtained for the energy valorization of syngas in a gas turbine, Case 2 and 3, are also presented in Tables 7 and 8. Due to the higher LHV obtained from syngas in Case 2, after the gasification process and the capture process, the amount of syngas needed to have a power of 5 MW is lower than in Case 1, by 3.85-7.28% depending on the plastic content in the mix.

Preprints (www.preprints.org) | NOT PEER-REVIEWED | Posted: 12 September 2023 doi:10.20944/preprints202309.0753.v1

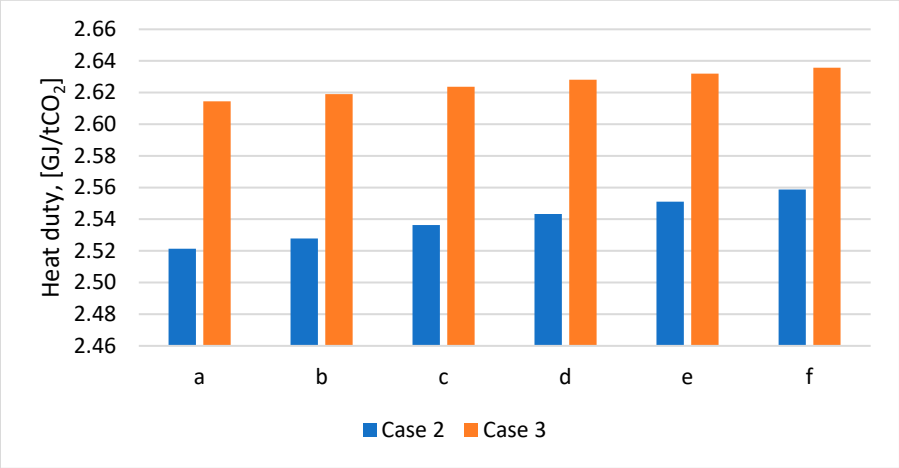

Figure 12. Variation of the heat duty according to PP content in the mix for Cases 2 and 3.

Table 7. Results of syngas use in a gas turbine – Case 2.

Case	2a	2b	2c	2d	2e	2f
Gas turbine power, MW	5	5	5	5	5	5
Syngas flow, kg/h	3 918.41	3 906.34	3 889.38	3 880.25	3 868.40	3 856.88
Air flow, kg/h	18 374.05	18 359.46	18 371.19	18 357.30	18 357.26	18 363.23
Combustion chamber temperature, °C	1 201.21	1 201.80	1 201.12	1 201.61	1 201.50	1 201.02
Flue gases temperature at the gas turbine outlet, °C	539.97	540.18	539.57	539.75	539.54	539.11
Flue gases flow, kg/h	22 292.47	22 265.81	22 260.58	22 237.57	22 225.08	22 220.13
L/G, [$kg_{solvent}/kg_{syngas}$]	0.64	0.57	0.51	0.46	0.42	0.38
Heat duty, GJ/tCO_2	2.521	2.528	2.536	2.543	2.551	2.559
Heat flow used for solvent regeneration, MJ/h	776	683	610	542	485	434
Water consumption CO_2 capture, kg/year	6 241.96	5 480.06	4 882.46	4 327.74	3 863.26	3 442.72
η_{GT}, %	39.89	40.03	40.16	40.26	40.35	40.44
η_{GGT}, %	32.7	32.8	32.96	33.08	33.19	33.28
Penalty efficiency, %	2.05	1.87	1.63	1.47	1.28	1.13
CO_2 emission factor, $kgCO_2/MWh$	889.28	878.06	866.01	856.04	845.93	837.13
Flue gases composition, wt. %						
H_2	0.02	0.02	0.02	0.02	0.02	0.02
O_2	13.32	13.32	133.3	13.32	13.32	13.33
N_2	74.00	74.07	74.14	74.20	74.27	74.32
CO_2	10.19	10.07	9.93	9.83	9.72	9.61
H_2O	2.46	2.52	2.57	2.63	2.67	2.72

Table 8. Results of syngas use in a gas turbine – Case 3.

Case	3a	3b	3c	3d	3e	3f
Gas turbine power, MW	5	5	5	5	5	5
Syngas flow, kg/h	4 226.19	4 166.87	4 122.22	4 079.09	4 046.16	4 011.36
Air flow, kg/h	18 105.73	18 166.44	18 181.29	18 213.95	18 214.20	18 243.19

Preprints (www.preprints.org) | NOT PEER-REVIEWED | Posted: 12 September 2023 doi:10.20944/preprints202309.0753.v1

Combustion chamber temperature, °C	1 202.88	1 201.25	1 201.68	1 201.06	1 201.89	1 201.19
Flue gases temperature at the gas turbine outlet, °C	543.71	542.15	541.99	541.20	541.38	540.62
Flue gases flow, kg/h	21 849.09	21 863.24	21 840.66	21 837.35	21 811.32	21 812.57
L/G, [$kg_{solvent}/kg_{flue\_gases}$]	0.93	0.91	0.89	0.87	0.86	0.84
Heat duty, GJ/tCO_2	2.614	2.619	2.624	2.628	2.632	2.636
Heat flow used for solvent regeneration, MJ/h	6 102	5 930	5 807	5 692	5 580	5 317
Water consumption CO_2 capture, kg/year	47 332.05	45 925.13	44 893.42	43 926.56	42 998.89	42 099.81
η_{GT}, %	32.19	32.40	32.54	32.68	32.81	33.13
η_{GGT}, %	27.27	27.47	27.62	27.75	27.88	28.14
Penalty efficiency, %	18.22	17.86	17.58	17.33	17.06	16.42
CO_2 emission factor, $kgCO_2/MWh$	96.63	95.41	91.73	88.49	87.88	87.33
Flue gases composition, wt. %						
H_2	0.02	0.02	0.02	0.02	0.02	0.02
O_2	13.32	13.38	13.40	13.44	13.44	13.47
N_2	74.56	74.73	74.88	75.02	75.14	75.24
CO_2	1.12	1.11	1.06	1.03	1.02	1.01
H_2O	10.93	10.72	10.58	10.45	10.33	10.20

After integration of the capture process, the net plant efficiency decreases due to the use of part of the energy produced in the regeneration process of the chemical solvent. In Case 2, the net plant efficiency penalty (η_{GGT}) is between 1.13-2.05%, and in Case 3, the η_{GGT} is between 16.42-18.22%. The significant difference in the cycle efficiency penalty between the two cases analysed (Case 2 and 3) is due to the amount of CO_2 that is removed from the treated gas stream; in Case 3, this amount is much higher. Figure 13 shows the comparative net plant efficiency ($\eta_{GT}$and η_{GGT}) for the three cases studied in cases a-f.

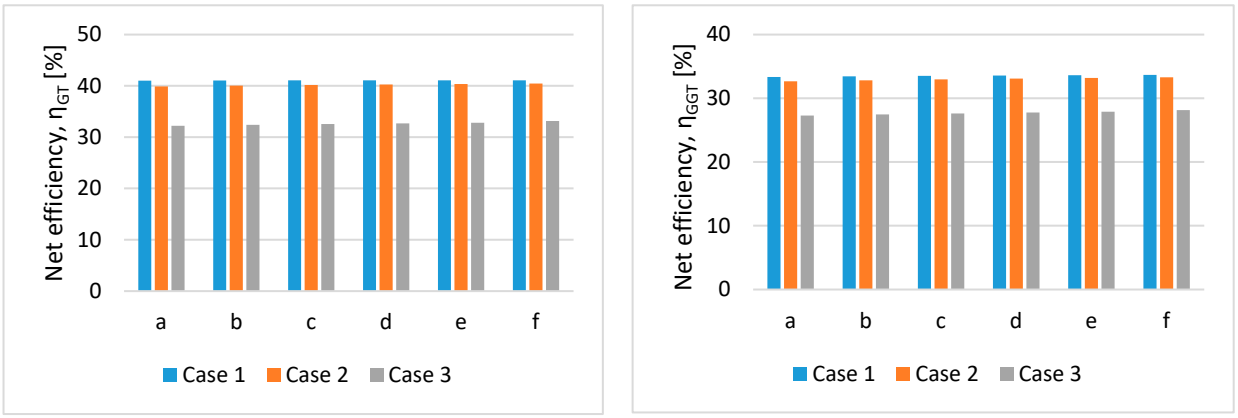

(**a**) (**b**)

Figure 13. Net plant efficiency depending on the mix used (η_{GT} - left)/ (η_{GGT} - right).

Figure 14 shows the CO_2 emission factor for the three cases in cases a-f. For Case 2, a CO_2 emission factor varied between 837.13-889.28 $kgCO_2/MWh$ was obtained, with 7.74-12.51% lower than in Case 1 because the syngas CO_2 content is negligible as comparing with post-combustion case. As for the CO_2 emission factor in Case 3, CO_2 emission factor decreases by about 90% compared to Case 1 due to the high amount of CO_2 content captured from flue gas. In Case 3, the main

Preprints (www.preprints.org) | NOT PEER-REVIEWED | Posted: 12 September 2023 doi:10.20944/preprints202309.0753.v1

disadvantage is the quantity of heat energy necessary in the solvent regeneration process, which is much higher than in Case 2 due to the more considerable CO_2 gas stream flow treated.

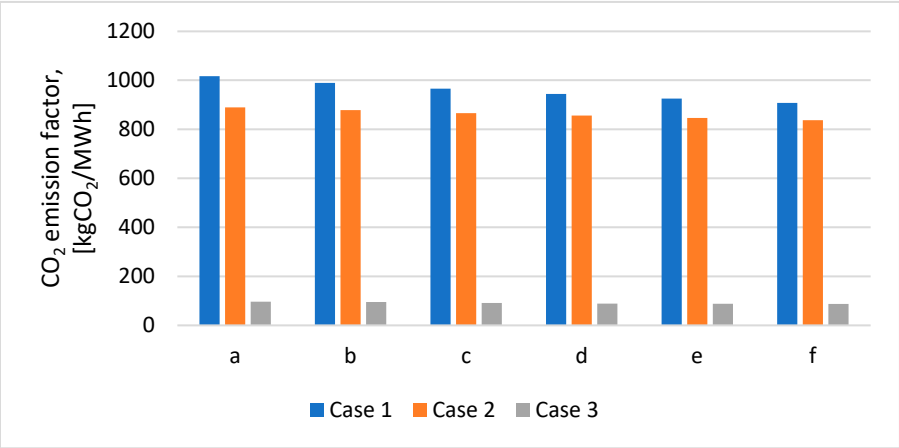

Figure 14. CO_2 emission factor depending on the mix used.

3.3. Negative CO_2 emissions

Biomass, a renewable energy source, is considered CO_2 neutral due to the CO_2 absorption in the growth process (photosynthesis process). Therefore, the CO_2 emissions generated during gasification and combustion processes according to poplar utilization are not considered in the CO_2 emission factor determination. Thus, the CO_2 emission factors for all three cases studied were recalculated, considering only the CO_2 emissions generated from plastic utilisation. The recalculated CO_2 emission factor was determined with equation 16, and the results are shown in Figure 15.

$$fCO_{2\_rec} = f_{CO2_{plastic}} - f_{CO2_{capture}}, [\frac{kg_{CO2}}{MWh}] \quad (16)$$

where: $f_{CO2_{plastic}}$ - represents the CO_2 emission factor for plastic, in $kgCO_2/MWh$; $f_{CO2_{capture}}$ - represents the CO_2 emission factor for poplar, in $kgCO_2/MWh$.

As compared to the initial assessment when all CO_2 emissions were taken into consideration, in Case 1, without CO_2 capture technology, the CO_2 emission factor was lower, 89.47%, for a 95% poplar content in the mix and 51.08% for a 70% poplar content in the mix. Further, by decreasing the poplar content in the mix, the CO_2 emissions increased because more plastic was used. In Case 2, only when 95% poplar was used in the mix a negative CO_2 emission of -6 $kgCO_2/MWh$ was obtained. In Case 3, when CAP post-combustion was integrated, for a poplar content in the mix between 75-95%, the CO_2 emission factor was negative varied between -84.94 and -716.16 $kgCO_2/MWh$. However, for 70% poplar content in the mix, the CO_2 emissions have slightly increased, being positive.

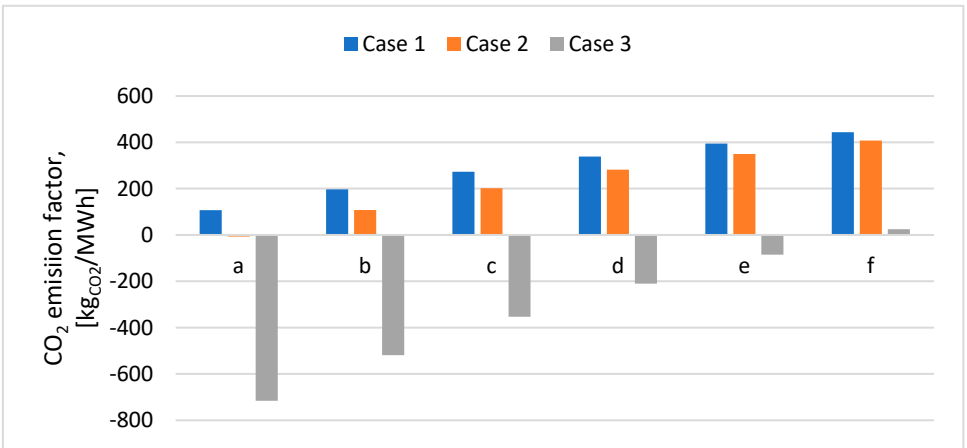

Figure 15. CO_2 emission factor depending on the mix used (poplar CO_2 neutral).

4. Conclusions

The optimal ER ratio considered was 0.35 for all cases studied. The proportion of PP in the feedstock mix varied between 5-30 % wt.. Considering that the CO_2 content ranged between 2.8-11.5% in syngas, the CAP integration's influence on the gas turbine energy system was studied. Monoethanolamine was used in a mass concentration of 30%, and the CO_2 capture efficiency considered was 90%. As expected, an increase in the LHV of the mixture was observed after the pre-combustion CO_2 capture process integration, as the proportion of plastic increased. The LHV varies between 5 269-5 532 kJ/kg (without CO_2 capture process) and 5 687-5 778 kJ/kg (with pre-combustion CO_2 capture process). Also, an increase in the H_2/CO ratio from 0.63 to 0.73 was observed as an increase of the plastic mass content in the mixture. The net plant efficiency was around 41%, with a CO_2 emission factor between 907.44-1 016.55 kgCO_2/MWh without the CO_2 capture process according to the PP content in the mix feed. By integrating the pre-combustion capture process, the net plant efficiency (η_{GGT}) decreases by 1.13-2.05% and the CO_2 emission factor by 7.74-12.51%. When post-combustion capture is integrated, net plant efficiency (η_{GGT}) decreases by 16.42-18.22% and the CO_2 emission factor by about 90%.

Author Contributions: Conceptualization, N.S and C.D.; methodology, N.S and C.D.; software, N.S and C.D.; validation, N.S and C.D.; formal analysis, N.S and C.D.; investigation, N.S and C.D.; resources, N.S and C.D.; data curation, N.S and C.D.; writing—original draft preparation, N.S and C.D.; writing—review and editing, N.S and C.D.; visualization, N.S and C.D.; supervision, N.S and C.D.; project administration, N.S and C.D.; funding acquisition, N.S and C.D. All authors have read and agreed to the published version of the manuscript.

Funding: This work was supported by EU Horizon 2020 (InNoPlastic), GA no. 10100061, and by the UEFISCDI within the National Project number 106PTE/2022. Additionally, the results presented in this article have been funded by the Ministry of Investments and European Projects through the Human Capital Sectoral Operational Program 2014-2020, Contract no. 62461/03.06.2022, SMIS code 153735.

Institutional Review Board Statement: Not applicable.

Informed Consent Statement: Not applicable.

Data Availability Statement: Not applicable.

Acknowledgments: N.S. acknowledges Academy of Romanian Scientists.

Conflicts of Interest: The authors declare no conflict of interest.

References

1. Antal, M. J.; Grønli, M. The art, science, and technology of charcoal production. *Ind. Eng. Chem. Res.* **2003**, 42.8, 1619–1640. https://doi.org/10.1021/ie0207919
2. Vasile, C.; Brebu, M. A. Thermal valorisation of biomass and of synthetic polymer waste. Upgrading of pyrolysis oils. *Cellul. Chem. Technol.*, **2006**, 40.7, 489–512.
3. Abnisa, F.; Daud, W. M. A. W. A review on co-pyrolysis of biomass: an optional technique to obtain a high-grade pyrolysis oil. *Energy Convers. Manag.* **2014**, 87, 71–85. https://doi.org/10.1016/j.enconman.2014.07.007
4. Varhegyi, G.; Antal Jr, M. J.; Szekely, T.; Szabo, P. Kinetics of the thermal decomposition of cellulose, hemicellulose, and sugarcane bagasse. *Energy Fuels*. **1989**, 3.3, 329–335. https://doi.org/10.1021/ef00015a012
5. Couhert, C.; Commandre, J. M.; Salvador, S. Is it possible to predict gas yields of any biomass after rapid pyrolysis at high temperature from its composition in cellulose, hemicellulose and lignin? *Fuel*. **2009**, 88.3, 408–417. https://doi.org/10.1016/j.fuel.2008.09.019
6. Kumar, R.. A review on the modelling of hydrothermal liquefaction of biomass and waste feedstocks. *Energy Nexus*. **2022**, 5, 100042. https://doi.org/10.1016/j.nexus.2022.100042
7. Jalili, M.; Ghasempour, R.; Ahmadi, M. H.; Chitsaz, A.; Holagh, S. G. An integrated CCHP system based on biomass and natural gas co-firing: Exergetic and thermo-economic assessments in the framework of energy nexus. *Energy Nexus*. **2022**, 5, 100016. https://doi.org/10.1016/j.nexus.2021.100016
8. Ciuffi, B.; Chiaramonti, D.; Rizzo, A. M.; Frediani, M.; Rosi, L. A critical review of SCWG in the context of available gasification technologies for plastic waste. *Appl. Sci.* **2020**, 10.18, 6307. https://doi.org/10.3390/app10186307
9. Badea, A. A.; Vodă, I.; Dincă, C. F. Comparative analysis of coal, natural gas and nuclear fuel life cycles by chains of electrical energy production. *U.P.B. Sci. Bull. Ser. C.* **2010**, 72.2, 221–238. https://www.scientificbulletin.upb.ro/rev_docs_arhiva/full8515.pdf

10. Dinca, C.; Badea, A. A.; Apostol, T.; Lazaroiu, G. GHG emissions evaluation from fossil fuel with CCS. Environ. *Eng. Manag. J.* **2009**, 8.1, 81–89.
11. Dinca, C.; Slavu, N.; Cormoş, C. C.; Badea, A. CO_2 capture from syngas generated by a biomass gasification power plant with chemical absorption process. *Energy*. **2018**, 149, 925–936. https://doi.org/10.1016/j.energy.2018.02.109
12. Block, C.; Ephraim, A.; Weiss-Hortala, E.; Minh, D. P.; Nzihou, A.; Vandecasteele, C. Co-pyrogasification of plastics and biomass, a review. *Waste Biomass Valor*. **2019**, 10.3, 483–509. https://doi.org/10.1007/s12649-018-0219-8
13. Sannigrahi, P.; Ragauskas, A. J.; Tuskan, G. A. Poplar as a feedstock for biofuels: a review of compositional characteristics. *Biofuels, Bioprod, Bioref.* **2010**, 4.2, 209–226. DOI: 10.1002/bbb.206
14. Yao, D.; Yang, H.; Chen, H.; Williams, P. T. Co-precipitation, impregnation and so-gel preparation of Ni catalysts for pyrolysis-catalytic steam reforming of waste plastics. *Appl. Catal. B.* **2018**, 239, 565–577. https://doi.org/10.1016/j.apcatb.2018.07.075
15. Cormos, C. C.; Dinca, C. Techno-economic and environmental implications of decarbonization process applied for Romanian fossil-based power generation sector. *Energy.* **2021**, 119734. https://doi.org/10.1016/j.energy.2020.119734
16. Ababneh, H.; AlNouss, A.; Al-Muhtaseb, S.A. Carbon Capture from Post-Combustion Flue Gas Using a State-Of-The-Art, Anti-Sublimation, Solid–Vapor Separation Unit. Processes 2022, 10, 2406. https://doi.org/10.3390/pr10112406
17. Dinca, C.; Badea, A.; Stoica, L.; Pascu, A. Absorber design for the improvement of the efficiency of post-combustion CO_2 capture. *J. Energy Inst.* **2015**, 88.3, 304–313. https://doi.org/10.1016/j.joei.2014.08.003
18. Sifat, N.S.; Haseli, Y. A Critical Review of CO_2 Capture Technologies and Prospects for Clean Power Generation. Energies 2019, 12, 4143. https://doi.org/10.3390/en12214143
19. Slavu, N.; Badea, A.; Dinca, C. Technical and Economical Assessment of CO_2 Capture-Based Ammonia Aqueous. Processes 2022, 10, 859. https://doi.org/10.3390/pr10050859
20. Pascu, A.; Stoica, L.; Dinca, C.; Badea, A. (2016). The package type influence on the performance of the CO2 capture process by chemical absorption. *U.P.B. Sci. Bull. Ser. C.* **2016**, 78.1, 259–270. https://www.scientificbulletin.upb.ro/rev_docs_arhiva/full409_910116.pdf
21. Peu, S.D.; Das, A.; Hossain, M.S.; Akanda, M.A.M.; Akanda, M.M.H.; Rahman, M.; Miah, M.N.; Das, B.K.; Islam, A.R.M.T.; Salah, M.M. A Comprehensive Review on Recent Advancements in Absorption-Based Post Combustion Carbon Capture Technologies to Obtain a Sustainable Energy Sector with Clean Environment. Sustainability 2023, 15, 5827. https://doi.org/10.3390/su15075827
22. Rajiman, V.; Hairul, N.A.H.; Shariff, A.M. Effect of CO_2 Concentration and Liquid to Gas Ratio on CO_2 Absorption from Simulated Biogas Using Monoethanolamine Solution. IOP Conf. Ser.: Mater. Sci. Eng. **2020**, 991(1), 012133. https://iopscience.iop.org/article/10.1088/1757-899X/991/1/012133
23. SGT-100 | Industrial Gas Turbine | Gas Turbines | Manufacturer | Siemens Energy Global. Available online: https://www.siemens-energy.com/global/en/offerings/power-generation/gas-turbines/sgt-100.html (accessed on 12 July 2023).